Lyapunov Drift-Plus-Penalty Based Resource Allocation in IRS-Assisted Wireless Networks with RF Energy Harvesting

Slavche PEJOSKI, Zoran HADZI-VELKOV, Tomislav SHUMINOSKI

Ss. Cyril and Methodious University in Skopje, 1000 Skopje, N. Macedonia

{slavchep, zoranhv, tomish}@feit.ukim.edu.mk

Submitted October 6, 2021 / Accepted June 20, 2022 / Online first August 3, 2022

Abstract. *We propose a resource allocation policy for intelligent reflective surface (IRS)-assisted wireless powered communication network (WPCN) where the energy harvesting (EH) users (EHUs) have finite energy storage and data buffers, for storing the harvested energy and the input (sensory) data, respectively. The IRS reflecting coefficients for uplink and downlink are chosen to focus the beam towards a specific EHU, but have additional constant phase offsets (different for uplink and downlink) in order to account for the direct link between the base station and the IRS targeted EHU, and the influence to the EH process of other EHUs in downlink. The EHUs acquire data from their sensors, receive energy in downlink and send information in uplink. We maximize the overall average amount of sensor information in the WPCN by optimizing the IRS reflecting coefficients for the downlink transmissions, the amount of acquired sensor information and the duration of the information transmission period for each EHU in each epoch using the Lyapunov drift-plus-penalty optimization technique. The simulation results demonstrate the effectiveness of the proposed solution.*

Keywords

Intelligent reflecting surfaces, Lyapunov drift-plus-penalty optimization, wireless powered networks

1. Introduction

The intelligent reflective surfaces (IRS) shape the multipath propagation in the radio channel in such a way to aid the communication between wireless transmitters and receivers. Thus, the IRS promises more efficient utilization of the available spectrum and energy budget [1–3]. The IRS consists of many sub-wavelength-sized elements that act as diffuse scatters combined together into a large metasurface [4]. In one of its many promising applications, the IRS can be merged together with wireless powered communications networks (WPCNs), which rely on radio frequency (RF) energy harvesting (EH) for charging the EH users (EHUs) [5], [6]. Namely, the EHUs, due to the physical limitations in their design and the rapid decrease of the available energy with distance, can harvest tiny amounts of energy. IRS can relay and focus the signal in both directions and thus increase the amount of harvested energy, together with the capacity of the wireless channel. The existing literature on IRS-assisted WPCNs typically optimize the phase shifts of each of the IRS antenna elements (meta elements) together with other resource allocation parameters [7–9]. The resource allocation schemes proposed so far typically rely on suboptimal iterative algorithms. These algorithms have high computational complexities that increase with the number of antenna elements, which makes them unsuitable for practical implementation. Namely, those algorithms are already computationally prohibitive for a few dozen IRS antenna elements, while current IRS implementations consist of few thousand in the experimental studies presented in [4], [10], and up to 10^4 IRS antenna elements in the experimental study in [11]. Recently a paper, [12], proposed a computationally simple beamforming solution, where the IRS beam is sequentially focused towards each EHU. The solution exploits the channel reciprocity and sets the same reflection matrix for the uplink and downlink transmissions. The paper has two model limitations: it assumes that during the EH process, the EHUs receive energy only when the IRS is aimed at them, and, it assumes that an obstacle exists between the base station (BS) and the EHUs that is not generally the case.

Most importantly, the previous works do not consider the sensory data acquisition process, the data storage available to the tiny wireless devices, and additionally do not control the energy levels of the EHU's battery. In this paper we are interesting in extending the system model from [12] to be able to adjust to a scenario where direct path between the BS and the EHUs exist, to correctly account for the receive energy in the slots where the IRS is not pointed to the designated EHU, and, based on the objective function optimize the IRS assisted EH process. This is achieved by offsetting the phases of the IRS elements with respect to simple focusing towards an EHU in the EH and information transmission (IT) phases of each user. Namely, the IRS phases in the IT

DOI: 10.13164/re.2022.0382

and EH parts will have constant phase offset for all IRS elements. Because of the mutual coupling between EHUs (due to the nature of the EH process), finding the constant phase offset for the EH phase is a non-convex problem and the approach presented in [12] is unable to find the solution. Here we aim to apply Lyapunov drift-plus-penalty method [13] which further accounts for buffer levels in both the data acquisition and the EH processes at the EHUs, and thus, brings the system model closer to reality.

This Lyapunov drift-plus-penalty optimization technique is a powerful technique for developing scheduling strategies for optimal utility performance of energy harvesting networks with finite capacity energy storage [14]. The use of Lyapunov drift-plus-penalty optimization technique is also appropriate for optimizing the operation of various communication networks where the queuing processes affect the system performance, for example, for improving average throughput and stabilizing the queuing in 5G nodes with vertical multi-homing capabilities [15] or optimizing the flow control and minimizing the energy consumption in stochastic networks [16] and [17]. The use of Lyapunov drift-plus-penalty techniques in WPCN have been studied in several papers [18–20]. The paper [18] considers the control of an energy self-sufficient receiver in a multi-access network with simultaneous wireless information and energy transfer. The authors in [19] consider an WPCN of body sensors that have limited energy and data buffer sizes. Similarly, [20] analyze a WPCN where the EHUs are equipped with finite energy buffers and data buffers but the BS is equipped with multiple antennas. Nonetheless, none of these papers considers the design of IRS assisted networks, nor the influence of IRS to the networks performance.

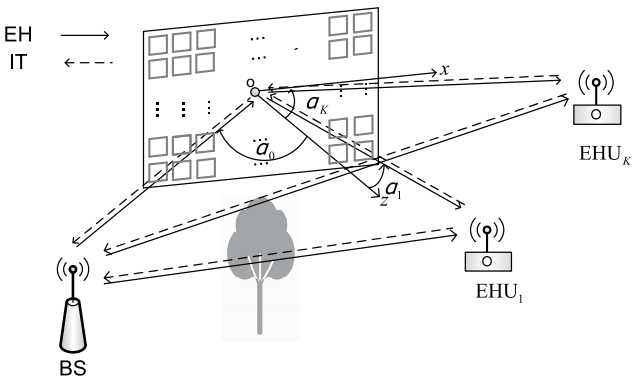

(a) System model.

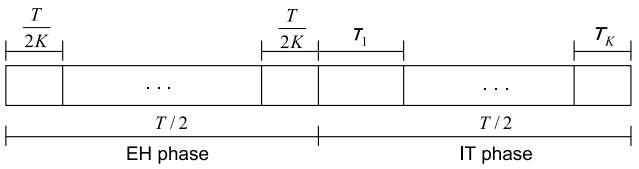

(b) TDMA frame organization.

Fig. 1. System model and TDMA frame organization.

In this paper we use the Lyapunov drift-plus-penalty optimization technique for resource allocation and parameters optimization in an IRS assisted WPCN consisting of EHUs with limited energy buffers and data buffers. The solution is of low complexity, can account for a direct communication link between BS and EHUs, takes into consideration the complete harvested energy, optimize the EH process and allows for maximizing the total amount of acquired sensory data in the WPCN. To the best of our knowledge, this is the first paper that introduces the Lyapunov drift-plus-penalty optimization technique for parameters optimization in IRS-assisted networks.

The paper is organized as follows: Section 2 introduces the communication system, Section 3 presents the optimization problem and its solution. Section 4 shows the numerical results and Section 5 concludes the paper.

2. System Model

We consider a WPCN with a single BS and K EHUs all equipped with a single antenna. All nodes employ TDMA and operate in half-duplex mode over the same frequency band. The IRS is deployed so as to maintain line of sights (LoS) to all nodes. On the other hand the BS can directly communicate with the different EHUs via a random fading channel without LoS. The BS transmits at fixed power P_0 and operates as an information receiver and an energy beacon. The EHUs transmit information to the BS. Additionally, each EHU is equipped with a sensors from which it collects the data that is transmitted in the IT phase. Each EHU is provisioned with a finite energy storage and a finite data buffer to store the harvested energy and to buffer the arrived data traffic (for example, due to sensory data acquisition), respectively. The system model is shown in Fig. 1 (a).

The communication session is divided into TDMA frames with unit durations $T = 1$ s and lasts M TDMA frames. Each TDMA frame is divided into two equal phases: an EH phase and an IT phase. Each phase is subdivided into K sub-slots. To aid simplicity of implementation, all sub-slots of the EH phase have equal durations, $T/(2K)$, and each sub-slot is allocated to a different EHU. In the IT phase of the tth TDMA frame, each EHU receives a slot of duration $\tau_k(t)T$ where $\tau_k(t)$ are the relative durations of the individual IT phases such that:

$$0 \leq \tau_k(t) \leq \frac{1}{2} \ \forall k, \tag{1}$$

$$\sum_{k=1}^{K} \tau_k(t) \leq \frac{1}{2}. \tag{2}$$

The system model is illustrated in Fig. 1 (b).

2.1 Channel Modeling

The IRS can be modeled as a planar antenna array consisting of N IRS antenna elements [3]. Assuming that each antenna element has an area of size A, such that $A \leq (\lambda/4)^2$, the total area can be calculated as $S = NA$. The IRS operation is controlled by its reflection matrix $\mathbf{\Theta} = \text{diag}(\text{e}^{\text{j}\theta_1}, \cdots, \text{e}^{\text{j}\theta_N})$. In $\mathbf{\Theta}$, $\theta_n \in [0, 2\pi)$ is the phase shift induced by the nth element of the IRS and it is assumed to be configurable and programmable via an IRS controller. During each sub-slot of the TDMA frame, the matrix $\mathbf{\Theta}$ is adjusted to the designated EHU. Namely, we assume that different IRS coefficients can be assigned during each sub-slot of each phase.

Due to the LoS assumption, the channel gain and the phase between the node and each IRS element are both fixed and deterministic. Thus, the BS-IRS channel is modeled by a deterministic vector $\mathbf{h} = [h_1, \cdots, h_N]^{\text{T}}$, where $h_n = \sqrt{\Omega_{0n}}\,\text{e}^{-\text{j}\phi_{0n}}$ is the channel between the BS and the nth antenna element of the IRS. Similarly, the IRS-kth EHU channel ($1 \leq k \leq K$) is represented by a deterministic vector, $\mathbf{g}_k = [g_{k1}, \cdots, g_{kN}]^{\text{T}}$, where $g_{kn} = \sqrt{\Omega_{kn}}\,\text{e}^{-\text{j}\phi_{kn}}$, Ω_{kn} is the channel gain and ϕ_{kn} is the phase between the kth EHU and the nth IRS element. Here, for analytical tractability, we assume that the IRS is a square surface whose center is placed at the origin of the coordinate system. In this case, the location of the nth antenna element is [3, Eq. (22), (23)]:

$$x_n = -\frac{(\sqrt{N}-1)\sqrt{A}}{2} + \sqrt{A}\text{mod}(n-1, \sqrt{N}), \tag{3}$$

$$y_n = -\frac{(\sqrt{N}-1)\sqrt{A}}{2} + \sqrt{A}\left\lfloor \frac{n-1}{\sqrt{N}} \right\rfloor. \tag{4}$$

For simplicity reasons and to obtain unambiguous notation, as shown in Fig. 1, we assume that all EHUs are located in the first quadrant, while the BS is located in the second quadrant. Thus, the BS is located at polar coordinates $(d_{\text{BS}}, -\alpha_0)$ with respect to (w.r.t) the origin and the z-axis, and so its angle w.r.t. the IRS boresight is α_0. Similarly, the kth EHU is located at polar coordinates (d_k, α_k). Thus, in our system model, the phases ϕ_{0n} and ϕ_{kn} are calculated as [3, Eq. (25)]:

$$\phi_{0n} = 2\pi\text{mod}\left(\frac{\sqrt{x_n^2 + y_n^2 + d_{\text{BS}}^2 - 2x_n d_{\text{BS}}\sin\alpha_0}}{\lambda}, 1\right), \tag{5}$$

$$\phi_{kn} = 2\pi\text{mod}\left(\frac{\sqrt{x_n^2 + y_n^2 + d_{\text{BS}}^2 - 2x_n d_k\sin\alpha_k}}{\lambda}, 1\right). \tag{6}$$

The values of the channel power gains in the general case when LoS is available are calculated as given with Lemma 1 from [3]. Nonetheless, for the case when both the BS and the EHUs operate in the far-field region of the IRS (defined by the inequality $S \leq 9d_{\text{BS}}^2$) their calculation is significantly simplified. Namely, Ω_{0n} are approximated by (c.f. [3, Eq. (11) and Eq. (31)])

$$\Omega_{0n} \approx \frac{A\cos(\alpha_0)}{4\pi d_{\text{BS}}^2} \equiv \Omega_0, \ \forall n \tag{7}$$

whereas channel gains of the kth EHU, Ω_{kn}, are approximated by

$$\Omega_{kn} \approx \frac{A\cos(\alpha_k)}{4\pi d_k^2} \equiv \Omega_k, \ \forall n. \tag{8}$$

In the kth sub-slot of the EH phase of the tth TDMA frame, the IRS aims to deliver most of the energy to the kth EHU by setting its reflection matrix, $\mathbf{\Theta}(k,t) = \text{diag}(\text{e}^{\text{j}\theta_1(k,t)}; \cdots; \text{e}^{\text{j}\theta_N(k,t)})$, with the phase shifts:

$$\theta_n(k,t) = \phi_{0n} + \phi_{kn} + \psi_k(t), \forall n. \tag{9}$$

This phase choice allows for focusing the the IRS beam towards the kth EHU as in [12]. But different form [12], the phase offset $\psi_k(t)$ in (9) is an additional phase that can account for the direct BS-kth EHU channel and can also influence the EH process at other EHUs in the kth sub-slot of the EH phase. Thus allowing other EHUs close to the kth EHU to harvest larger amounts of RF energy that effectively can lead to broadening of the EH region around the kth EHU.

The direct channel between the BS and the kth EHU is modeled as block fading channel with random gain h_{dk} (with amplitude $|h_{dk}|$ and a random phase ϕ_{dk} i.e. $h_{dk} = |h_{dk}|\text{e}^{-\text{j}\phi_{dk}}$), where the average power gain of the channel is $\Omega_{dk} = \mathbb{E}\left[|h_{dk}|^2\right]$.

2.2 Data Queue and Transmission Model

Let the maximum amount of inbound data, during one frame, be denoted by $i_{k,\max}$, and the instantaneous amount of inbound data be denoted by $i_k(t)$. Then the data acquired by the kth EHU (e.g., from the sensory measurements) during frame t is given by:

$$0 \leq i_k(t) \leq i_{k,\max}. \tag{10}$$

The data transmitted by the kth EHU in the IT phase of the tth frame is calculated as:

$$o_k(t) = \tau_k(t)TW\log_2\left(1 + \frac{P_k|\mathbf{h}^{\text{T}}\mathbf{\Theta}_{\text{IT}}(k,t)\mathbf{g}_k + h_{dk}(t)|^2}{N_0 W}\right) \tag{11}$$

where W is the bandwidth of the WPCN. From (11) it is obvious that during the IT phase, the IRS reflection matrix in the kth sub-slot do not influence the rate of other EHUs (namely, the information sent by the kth EHU is of interest only to the BS). Thus, to maximize $o_k(t)$, without spending any additional resources, the phases in $\mathbf{\Theta}_{\text{IT}}(k,t)$ should be chosen as [3]:

$$\theta_{n,\text{IT}}(k,t) = \phi_{0n} + \phi_{kn} - \phi_{dk}(t), \forall n \tag{12}$$

which aligns the phases of the IRS assisted beam and the direct path between the kth EHU and the BS, and thus provides maximum SNR at the BS.

Denoting $D_k(t)$ to be the length of the data queue of the kth EHU at the beginning of the frame t, the dynamics of the data queue is described by:

$$D_k(t+1) = \max\left[D_k(t) - o_k(t), 0\right] + i_k(t). \tag{13}$$

2.3 Energy Harvesting and Consumption Model

Each EHU is equipped with an rechargeable battery with fixed energy storage capacity denoted by Λ_k. In this paper we assume that EHUs transmit at a very low power levels and that the distance between the EHUs are such that the harvested energy during the IT phase is negligible. During the uth sub-slot of the EH phase, the kth EHU harvests energy of the amount $\eta_k \frac{T}{2K} P_0 |\mathbf{h}^{\mathrm{T}} \mathbf{\Theta}_{\mathrm{EH}}(u,t)\mathbf{g}_k + h_{dk}(t)|^2$, where η_k is the EH efficiency of the kth EHU. Thus, the amount of energy harvested by the kth EHU during the EH phase is:

$$e_k^{\mathrm{in}}(t) = \frac{\eta_k P_0 T}{2K} \sum_{u=1}^{K} |\mathbf{h}^{\mathrm{T}} \mathbf{\Theta}_{\mathrm{EH}}(u,t)\mathbf{g}_k + h_{dk}(t)|^2. \quad (14)$$

Please note that the choice of $\mathbf{\Theta}_{\mathrm{EH}}(u,t)$ for $u = 1, ..., K$ impacts $e_k^{\mathrm{in}}(t)$, unlike $\mathbf{\Theta}_{\mathrm{IT}}(u,t)$ that does not affect $o_k(t)$ for $u \neq k$. This justifies the need for different IRS matrices for the sub-slots of the same EHU during the IT and EH phases.

The energy spent by the kth EHU, $e_k^{\mathrm{out}}(t)$, is determined by the power consumption of the sensory data acquisition and the power consumption of the RF information transmission, as:

$$e_k^{\mathrm{out}}(t) = \epsilon_k i_k(t) + P_k \tau_k(t) T \quad (15)$$

where ϵ_k is the energy consumption per one bit of data acquired by the kth EHU sensor and P_k is the transmit RF power of the kth EHU. We assume that P_k is predetermined constant parameter associated with the hardware settings of the kth EHU.

Based on the EH and the energy consumption model, the length of the energy queue at the kth EHU in the tth frame is $E_k(t)$ and its dynamics, can be described as:

$$E_k(t+1) = \min[E_k(t) + e_k^{\mathrm{in}}(t) - e_k^{\mathrm{out}}(t), \Lambda_k]. \quad (16)$$

3. Resource Allocation

Similar to [19] and [20], our proposed scheme is designed by maximizing the average amount of acquired sensory data by all the EHUs in the WPCN:

$$\underset{i_k(t),\psi_k(t),\tau_k(t)}{\text{Maximize}} \lim_{M->\infty} \frac{1}{M} \sum_{t=0}^{M-1} \sum_{k=1}^{K} i_k(t). \quad (17)$$
$$\text{s.t.} \quad (1), (2), (9) - (16)$$

The optimization problem (17) is non-convex problem due to the the constraint associated with (14) which is non-convex with respect to $\psi_k(t)$, $\forall k$. In order to solve (17) we resort to the Lyapunov-drift-plus penalty (LDPP) method [13]. The LDPP method guarantees stability of the energy and data queues, $E_k(t)$ and $D_k(t)$ respectively. Namely, using (13), (16) and the assumption that both buffers are limited in capacity it can be easily shown that they are stable [13]. The method consists of defining the Lyapunov function based on the queuing model, finding the upper bound on the LDPP function and sub-optimally minimizing it under the constraints of the original problem, independently in each TDMA epoch.

Let us denote the state of the energy queue by $\mathbf{E}(t) = [E_1(t), ..., E_K(t)]^{\mathrm{T}}$ and the state of the energy queue by $\mathbf{D}(t) = [D_1(t), ..., D_K(t)]^{\mathrm{T}}$. Then, the queue vector is defined as $\mathbf{S}(t) = [\mathbf{D}(t), \mathbf{E}(t)]^{\mathrm{T}}$. The Lyapunov function is defined to evaluate the length of the data queue $D_k(t)$ and the free space of battery $\Lambda_k - E_k(t)$ [19] as:

$$L(\mathbf{S}(t)) = \frac{1}{2}\left[\sum_{k=1}^{K} \mu_{1k} D_k^2(t) + \mu_{2k}(\Lambda_k - E_k(t))^2\right] \quad (18)$$

where μ_{1k} and μ_{2k} are nonnegative constants used to balance among the different nature of the buffers [20]. Please note that by minimizing $L(\mathbf{S}(t))$ the data buffer can approach to an empty state level, and the energy queue can approach a level of Λ_k.

The one-step conditional Lyapunov drift is defined as:

$$\Delta(\mathbf{S}(t)) = \mathbb{E}\left\{L(\mathbf{S}(t+1)) - L(\mathbf{S}(t)) \mid \mathbf{S}(t)\right\}. \quad (19)$$

The Lyapunov drift-plus-penalty expression is defined as:

$$\Delta(\mathbf{S}(t)) - V \cdot \mathbb{E}\left\{\sum_{k=1}^{K} i_k(t) \mid \mathbf{S}(t)\right\} \quad (20)$$

where V is a nonnegative control parameter.

The LDPP method seeks to minimize the upper bound of (20), in each t, for all possible values of the state $\mathbf{S}(t)$, and for all control parameters $V > 0$. By expanding (19), we obtain

$$\begin{aligned}\Delta(\mathbf{S}(t)) =& \frac{1}{2}\mathbb{E}\left\{\sum_{k=1}^{K}\Big(\mu_{1k}(D_k^2(t+1) - D_k^2(t)) \right.\\ &+ \mu_{2k}((\Lambda_k - E_k(t+1))^2 \\ &\left. -(\Lambda_k - E_k(t))^2)\Big) \mid \mathbf{S}(t)\right\}.\end{aligned} \quad (21)$$

Using (16) we easily obtain $(\Lambda_k - E_k(t+1))^2 = (\min[E_k(t) + e_k^{\mathrm{in}}(t) - e_k^{\mathrm{out}}(t) - \Lambda_k, 0])^2$. Applying the inequality $(\min[a,0])^2 \leq a^2$ we obtain:

$$\begin{aligned}(\Lambda_k - E_k(t+1))^2 &\leq (E_k(t) + e_k^{\mathrm{in}}(t) - e_k^{\mathrm{out}}(t) - \Lambda_k)^2 \\ &\leq (E_k(t) - \Lambda_k)^2 + e_k^{\mathrm{in}}(t)^2 + e_k^{\mathrm{out}}(t)^2 \\ &- 2(E_k(t) - \Lambda_k)(e_k^{\mathrm{out}}(t) - e_k^{\mathrm{in}}(t)).\end{aligned} \quad (22)$$

Similarly, using (13) we obtain $D_k^2(t+1) = (\max[D_k(t) - o_k(t), 0] + i_k(t))^2$. Additionally expanding $D_k^2(t+1)$, using $(\max[a,0])^2 \leq a^2$ and $\max[c-d,0] < c$ for nonnegative a, c and d, we obtain:

$$\begin{aligned}D_k^2(t+1) &\leq (D_k(t) - o_k(t))^2 + i_k(t)^2 \\ &+ 2\max[D_k(t) - o_k(t), 0]\, i_k(t) \\ &\leq (D_k(t) - o_k(t))^2 + i_k(t)^2 + 2D_k(t) i_k(t).\end{aligned} \quad (23)$$

Introducing (22) and (23) in (21) and (20), and noticing that all parameters in (20) are non-negative, the one-step conditional LDPP expression from (20) is upper bounded by:

$$\begin{aligned}
&\Delta(\mathbf{S}(t)) - V \cdot \mathbb{E}\left\{\sum_{k=1}^{K} i_k(t) \mid \mathbf{S}(t)\right\} \\
&\leq U + \mathbb{E}\left\{\sum_{k=1}^{K} \mu_{2k}(E_k(t) - \Lambda_k) e_k^{\text{in}}(t) \mid \mathbf{S}(t)\right\} \\
&+ \mathbb{E}\left\{\sum_{k=1}^{K} (\mu_{1k} D_k(t) - \mu_{2k}\epsilon_k(E_k(t) - \Lambda_k)) i_k(t) \mid \mathbf{S}(t)\right\} \\
&- V \cdot \mathbb{E}\left\{\sum_{k=1}^{K} i_k(t) \mid \mathbf{S}(t)\right\} \\
&- \mathbb{E}\left\{\sum_{k=1}^{K} \mu_{1k} D_k(t) o_k(t) + \mu_{2k}(E_k(t) - \Lambda_k) P_k \tau_k(t) T \mid \mathbf{S}(t)\right\}
\end{aligned} \tag{24}$$

where U is a finite constant related to the worst-case second moments of $o_k(t)$, $i_k(t)$, $e_k^{\text{in}}(t)$, and $e_k^{\text{out}}(t)$ processes, i.e.:

$$\begin{aligned}
U = \frac{1}{2}\mathbb{E}\Bigg\{&\sum_{k=1}^{K} \mu_{1k}(o_k(t)^2 + i_k(t)^2) \\
&+ \mu_{2k}(e_k^{\text{in}}(t)^2 + e_k^{\text{out}}(t)^2) \mid \mathbf{S}(t)\Bigg\}
\end{aligned} \tag{25}$$

and is of no importance to the optimization process [13].

The LDPP method minimizes the right-hand-side of the inequality (24) (after removing U), by choosing the most appropriate control policy action in each epoch. This leads to removing the averaging from the right hand side of (24), dropping U and minimizing it under the constraints from (17). Please note that in (24) there are three different parts:

- the part $\sum_{k=1}^{K} \mu_{2k}(E_k(t) - \Lambda_k) e_k^{\text{in}}$, affected by the EH process and the IRS configuration (in our optimization problem influenced by $\psi_k(t)$), is called IRS configuration sub-problem;
- the second part is $\sum_{k=1}^{K} (\mu_{1k} D_k(t) - \mu_{2k}\epsilon_k(E_k(t) - \Lambda_k)) i_k(t) - V \sum_{k=1}^{K} i_k(t)$, which depends on $i_k(t)$, and, is termed data acquisition sub-problem;
- the third part $-\sum_{k=1}^{K} \mu_{1k} D_k(t) o_k(t) + \mu_{2k}(E_k(t) - \Lambda_k) P_k \tau_k(t) T$, which depends on $\tau_k(t)$, is the information transmission sub-problem.

Please note that even for more complex optimization problems with more variables, the same sub-problem structure remains [20].

3.1 IRS Configuration Sub-Problem

The IRS configuration sub-problem is formulated as:

$$\min_{\psi_k(t)} \sum_{k=1}^{K} \mu_{2k}(E_k(t) - \Lambda_k) e_k^{\text{in}}. \tag{26}$$

Due to (16) we have $(E_k(t) - \Lambda_k) \leq 0 \ \forall k$. The problem can be solved by setting the first derivative of the objective function of (26) with respect to variable $\psi_k(t)$ to zero, and finding the root of the resulting transcendental equation, which yields:

$$\psi_k(t) = \text{atan}\left(\frac{-\sum_{j=1}^{K} \mu_{2j}\eta_j \Delta E_j(t) |B_{j,k} h_{dj}(t)| \sin(\phi_{dj}(t) + \Delta\phi_{j,k})}{\sum_{j=1}^{K} \mu_{2j}\eta_j \Delta E_j(t) |B_{j,k} h_{dj}(t)| \cos(\phi_{dj}(t) + \Delta\phi_{j,k})}\right) \tag{27}$$

where $\Delta E_j(t) = \Lambda_j - E_j(t)$, $B_{j,k} = |B_{j,k}| e^{\mathrm{j}\Delta\phi_{j,k}} = \mathbf{h}^{\mathrm{T}} \boldsymbol{\Theta}^0(j,t) \mathbf{g}_k$ and $\boldsymbol{\Theta}^0(j,t)$ is obtained from $\boldsymbol{\Theta}(j,t)$ when $\psi_k(t) = 0$ in (9).

3.2 Data Acquisition Sub-Problem

The Data acquisition sub-problem is given by:

$$\min_{i_k(t)} \sum_{k=1}^{K} (\mu_{1k} D_k(t) + \mu_{2k}\epsilon_k(\Lambda_k - E_k(t)) - V) i_k(t). \tag{28}$$
$$\text{s.t.} \quad (10)$$

Problem (28) is constrained linear problem and its solution is:

$$i_k(t) = \begin{cases} i_{k,\max}, & V \geq \mu_{1k} D_k(t) + \mu_{2k}\epsilon_k(\Lambda_k - E_k(t)) \\ 0, & V < \mu_{1k} D_k(t) + \mu_{2k}\epsilon_k(\Lambda_k - E_k(t)) \end{cases} \tag{29}$$

3.3 Information Transmission Sub-Problem

The information transmission sub-problem is given as:

$$\min_{\tau_k(t)} -\sum_{k=1}^{K} \mu_{1k} D_k(t) o_k(t) + \mu_{2k}(E_k(t) - \Lambda_k) P_k \tau_k(t) T. \tag{30}$$
$$\text{s.t.} \quad (1) \text{ and } (2)$$

Problem (30) is a convex problem with closed form solution given by:

$$\tau_k(t) = \begin{cases} 1/2, & k = \text{argmax}_u Q(u) \text{ and } ff(k) > 0 \\ 0, & \text{otherwise} \end{cases} \tag{31}$$

where $Q(u) = \mu_{1u} D_u(t) W \log_2\left(1 + \frac{P_u |\mathbf{h}^{\mathrm{T}} \boldsymbol{\Theta}_{\text{IT}}(u,t) \mathbf{g}_u + h_{du}(t)|^2}{N_0 W}\right) - \mu_{2u}(\Lambda_u - E_u(t)) P_u$.

3.4 LDPP Method Resource Allocation

The LDPP method for our paper is named IRS aware LDPP algorithm (ILA). Using (27), (29), (31) and the equations (13) and (16) describing the dynamics of the buffers, the complete ILA algorithm is shown in Algorithm 1.

Algorithm 1. ILA Algorithm.

Initialize: $D_k(0)$, $E_k(0)$ $\forall k$. Set $t = 1$;
repeat
  Step 1: Choose $\psi_k(t)$ based on (27)
  Step 2: Choose $i_k(t)$ based on (29)
  Step 3: Choose $\tau_k(t)$ based on (31)
  Step 4: Update $D_k(t)$ based on (13)
  Step 5: Update $E_k(t)$ based on (16)
  Step 6: Set $t = t + 1$
until $t \leq M$

4. Numerical Results

In this section, we illustrate the performance of the ILA algorithm presented in Algorithm 1, termed "Proposed ILA algorithm".

The area of each IRS antenna element is set to $A = (\lambda/4)^2$ with $\lambda = 0.1$ m (corresponding to the carrier frequency of 3 GHz). The IRS consists of $N = 2500$ IRS antenna elements. The BS transmit power is set to $P_0 = 4$ W, and the BS thermal noise power density is set to $N_0 = 10^{-19}$ W/Hz. The BS is placed at an angle of $\alpha_0 = \pi/4$. The EHUs are uniformly distributed along an arc of radius d_k within a range of polar angles from $\pi/6$ to $\pi/3$. For the direct path, we assume that the average power gain depends on the distance as $\Omega_{dk} = 10^{-3} d_{dk}^{-3}$, where d_{dk} is the distance of the direct path between the BS and the kth EHU (d_{dk} is calculated based on d_{BS}, d_k, α_0 and α_k using the cosine theorem).

The capacity of the data buffers of each EHU is set to 10^9 bits, whereas the capacity of the energy buffer of each EHU is set to $\Lambda_k = 1$ J. The initial values for the energy and data buffers are set to 10% of their maximum value. The number of TDMA frames is set to $M = 10^6$ and $\eta_k = 0.9\ \forall k$.

Firstly, we compare the performance of the proposed algorithm with a corresponding scheme based on conventional convex optimization developed in [12] (denoted by the "Benchmark IRS"). The BS and the EHUs are placed along an arc centered at the IRS with radius $d_{\mathrm{BS}} = d_k = 15$ m. It is assumed that the radiation pattern of the IRS in the benchmark is independent of the angle between the IRS and its LoS to the corresponding node. Note, since all EHUs are at same distance from the IRS, the max-min resource allocation considered in [12] reduces to the max-sum-rate resource allocation that corresponds to the objective function of the resource allocation problem (17). Note, the scheme considered in [12] assumes that the IRS can attain a very narrow beam aimed exactly at the targeted EHU, such that other EHUs cannot harvest RF energy outside their dedicated EH sub-slots.

Additionally, to facilitate a fair comparison, we set $\Omega_{kd} = 0$, as the benchmark scheme ignores the direct LoS between BS and EHUs. Since the benchmark scheme also ignores the information acquisition process, such that the sensory data is always available to the EHUs, we also set $\epsilon_k = 0$, $\forall k$. Additionally, to ensure that the acquired data is equal to the transmitted data we choose V, μ_1 and μ_2 to keep the buffers in "Proposed ILA algorithm" at levels very close to their initial levels. The transmit power of the EHUs was set to 4 µW and the communication channel bandwidth was set to 1 MHz. As a performance metric, we adopt the system's sum achievable rate which for the "Proposed ILA algorithm" is defined by:

$$R_{\mathrm{sum}} = \frac{1}{W}\frac{1}{M}\sum_{k=1}^{K}\sum_{t=0}^{M-1} i_k(t).$$

The performance comparison is shown in Fig. 2. Figure 2 shows that our proposed scheme significantly outperforms the benchmark for $K \geq 10$. The performance gap between the proposed and the benchmark scheme increases with increasing the number of EHUs, K. In the proposed scheme, as K increases, the distance among EHUs decreases, the amount of harvested energy by the neighboring EHUs in a given EH sub-slot increases, and, thus, the sum achievable rate increases. On the other hand, the performance of the benchmark scheme is independent of K, because its problem formulation assumes that during a given EH sub-slot, only one specific EHU collects the broadcasted RF energy through the IRS, while the other EHUs do not collect RF energy no matter how close they are to the EHU to which the beam is directed.

Next, we compare "Proposed ILA algorithm" for three different system settings: 1. "Symmetric IRS assisted WPCN", 2. "IRS assisted WPCN" and 3. "WPCN without IRS", respectively. Specifically, "Symmetric IRS assisted WPCN" is obtained when $\boldsymbol{\Theta}_{\mathrm{EH}}(k,t)$ is the same as $\boldsymbol{\Theta}_{\mathrm{IT}}(k,t)$ i.e. $\psi_k(t) = -\phi_{dk}(t)$. The "IRS assisted WPCN" is obtained when in Step 1 of Algorithm 1, the value of $\psi_k(t)$ is set to $\psi_k(t) = 0$. This gives a simple focusing of the IRS beam towards EHU k but doesn't consider for the influence of the BS-EHU k direct path. The setting "WPCN without IRS" is obtained when no IRS is present. We specifically study the average sum of the acquired data:

$$I_{\mathrm{sum}} = \frac{1}{M}\sum_{k=1}^{K}\sum_{t=0}^{M-1} i_k(t).$$

We set $\mu_{1k} = 1.6 \times 10^{-10}$ and $\mu_{2k} = 5 \times 10^{12}$. If not stated otherwise we set $V = 10000$. Also, the maximum amount of collected data at the sensors is set to $i_{k,\max} = 10$ kbit $\forall k$, and, the monitoring power consumption is set to $\epsilon_k = 0.01$ mJ/kbit $\forall k$ as in [19] and [21], which corresponds to acquisition rates for temperature, glucose and accelerometer and the typical acquisition power consumption. Additionally, the transmission power of each EHU is set to $P_k = 20$ nW $\forall k$. The bandwidth of the communication session is set to 100 kHz and $d_k = 5$ m $\forall k$.

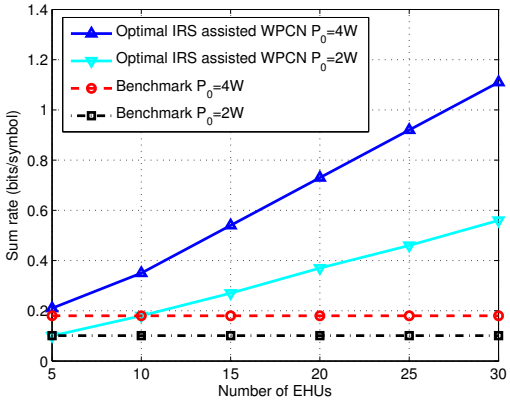

Fig. 2. The sum rate R_{sum} v.s. the number of EHUs.

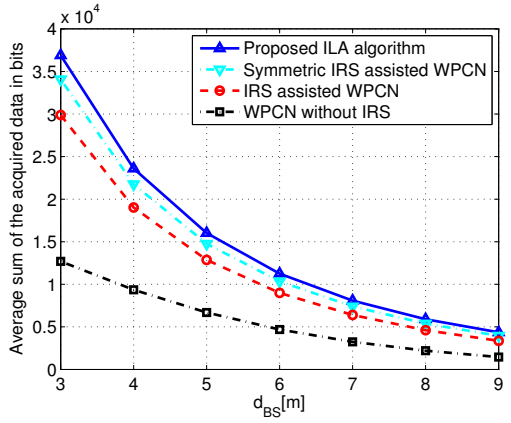

Fig. 3. The average sum of the acquired data I_{sum} v.s. d_{BS} for $K = 15$.

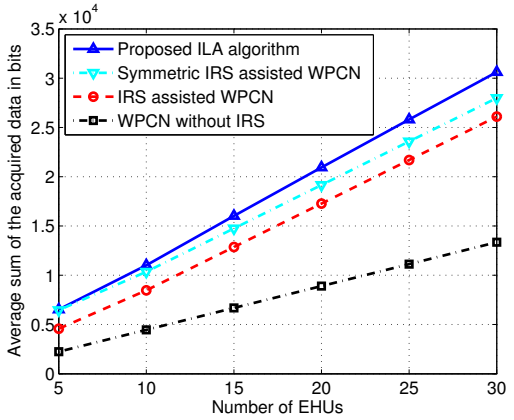

Fig. 4. The average sum of the acquired data I_{sum} v.s. K for $d_{\text{BS}} = 5$ m.

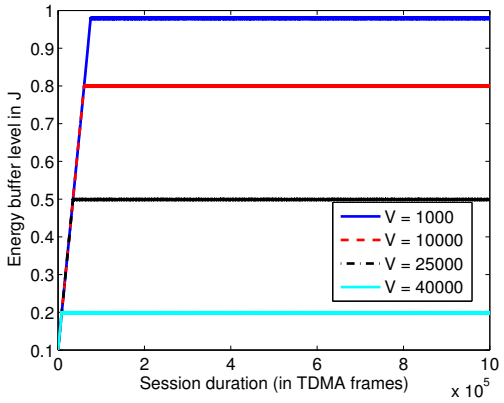

(a) Energy buffer.

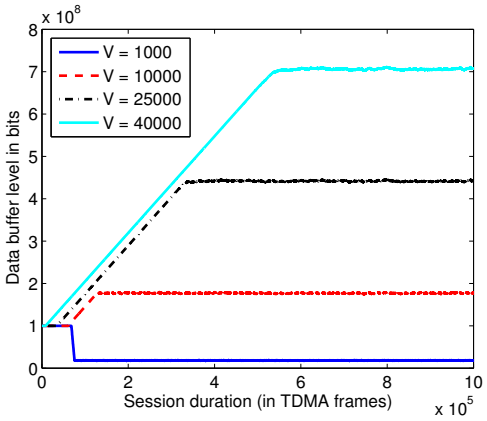

(b) Data buffer.

Fig. 5. The energy and data buffers for the EHU with $k = 1$ for the session duration parametrized with different values of V for $K = 15$.

Figure 3 shows the I_{sum} as a function of d_{BS}. With the increase in d_{BS} the average sum of the acquired data is reduced. For the considered scenario, the introduction of IRS increases the I_{sum} approximately twice, and the optimal choice of $\psi_k(t)$ increases I_{sum} for approximately another 50% compared to the "WPCN without IRS". The optimal choice of $\psi_k(t)$ leads to performance improvement compared to the choice $\psi_k(t) = -\phi_{dk}(t)$ which justifies the different IRS reflection matrices for uplink and downlink.

In Fig. 4, the average sum of the acquired data for different number of EHUs is shown. The increase in the number of EHUs increases I_{sum}. "Proposed ILA algorithm" due to its awareness for the influence of the EH phase of one EHU to the EH process of other EHUs allows for highest value of I_{sum} over the whole considered range of K.

In Fig. 5, the energy and data buffer levels of the EHU with $k = 1$ for the session duration are shown. The results in the figure are parametrized for different values of V. It should be noted that similar figures with small variations can be found for the EHUs with different values of k. We have found that for the analyzed scenario, the values for V can range from 1000 to 45000 for the buffers to be away from overloading or emptying. Nonetheless, those ranges for V should be observed in correlation with μ_{1k}, μ_{2k} and the analyzed scenario. In Fig. 5 three regions in the figures can be observed. In the first region the EHU energy buffer approaches its steady level, in the second region, the data buffer approaches its steady level, and in the third region both buffers are at their steady levels. The figures show that the increase in V leads to increase in the data buffer level, and decrease in the energy buffer level. This comes from the chosen Lyapunov function in (18). Namely, for small values of V, the influence of the Lyapunov drift in (24) is stronger than the penalty influence. Thus, the buffers are closer to the values obtained by just minimizing the Lyapunov function. As V increases the penalty becomes more important and the buffer levels move in opposite direction.

5. Conclusion and Future Work

The paper uses the Lyapunov drift-plus-penalty optimization technique for resource allocation and IRS parameters optimization in an IRS assisted wireless powered communication networks, composed of EHUs with limited energy buffers and data buffers. The provided solution is of low complexity, can be used in presence of a direct communication link between BS and EHUs, optimizes the IRS assisted EH process and maximizes the average acquired sensory data.

By presenting the average sum of the acquired data for different numbers of EHUs and for different positions of the base station the paper shows the superiority of the optimal solution compared to the benchmarks. Additionally, by presenting the energy and data buffers for the EHUs, it is shown that the increase in the control parameter V leads to increasing of the data buffer level, and to decrease in the energy buffer level. In our future work we will develop enhanced resource allocation schemes for more practical communication systems, including multi-antenna BS, non-orthogonal multiple access (NOMA), and active IRS vs. passive IRS comparison.

References

[1] BASAR, E., RENZO, M. D., ROSNY, J. D., et al. Wireless communications through reconfigurable intelligent surfaces. *IEEE Access*, 2019, vol. 7, p. 116753–116773. DOI: 10.1109/ACCESS.2019.2935192

[2] WU, Q., ZHANG, R. Towards smart and reconfigurable environment: intelligent reflecting surface aided wireless network. *IEEE Communications Magazine*, 2020, vol. 58, no. 1, p. 106–112. DOI: 10.1109/MCOM.001.1900107

[3] BJORNSON, E., SAGUINETTI, L. Power scaling laws and near-field behaviors of massive MIMO and intelligent reflecting surfaces. *IEEE Open Journal of the Communications Society*, 2020, vol. 1, p. 1306–1324 . DOI: 10.1109/OJCOMS.2020.3020925

[4] RENCO, M. D., ZAPPONE, A., DEBBAH, M., et al. Smart radio environments empowered by reconfigurable intelligent surfaces: how it works, state of research, and the road ahead. *IEEE Journal on Selected Areas in Communications*, 2020, vol. 38, no. 11, p. 2450–2525. DOI: 10.1109/JSAC.2020.3007211

[5] KRIKIDIS, I., TIMOTHEOU, S., NIKOLAOU, S., et al. Simultaneous wireless information and power transfer in modern communication systems. *IEEE Communications Magazine*, 2014, vol. 52, no. 11, p. 104–110. DOI: 10.1109/MCOM.2014.6957150

[6] PEJOSKI, S., HADZI-VELKOV, Z., SCHOBER, R. Optimal power and time allocation for WPCNs with piece-wise linear EH model. *IEEE Wireless Communications Letters*, 2018, vol. 7, no. 3, p. 364–367. DOI: 10.1109/LWC.2017.2778146

[7] ZHENG, Y., BI, S., ZHANG, Y. J., et al. Intelligent reflecting surface enhanced user cooperation in wireless powered communication networks. *IEEE Wireless Communications Letters*, 2020, vol. 9, no. 6, p. 901–905. DOI: 10.1109/LWC.2020.2974721

[8] WU, Q., ZHANG, R. Weighted sum power maximization for intelligent reflecting surface aided SWIPT. *IEEE Wireless Communications Letters*, 2020, vol. 9, no. 5, p. 586–590. DOI: 10.1109/LWC.2019.2961656

[9] LYU, B., HOANG, D. T., GONG, S., et al. Intelligent reflecting surface assisted wireless powered communication networks. In *Proceeding of WCNC Workshops 2020*. Seoul (Korea), 2020, p. 1–6. DOI: 10.1109/WCNCW48565.2020.9124775

[10] HU, J., ZHANG, H., DI, B., et al. Reconfigurable intelligent surface based RF sensing: Design, optimization, and implementation. *IEEE Journal on Selected Areas in Communications*, 2020, vol. 38, no. 11, p. 2700–2716. DOI: 10.1109/JSAC.2020.3007041

[11] TANG, W., CHEN, M. Z., CHEN, X., et al. Wireless communications with reconfigurable intelligent surface: Path loss modeling and experimental measurement. *IEEE Transactions on Wireless Communications*, 2021, vol. 20, no. 1, p. 421–439. DOI: 10.1109/TWC.2020.3024887

[12] HADZI-VELKOV, Z., PEJOSKI, S., ZLATANOV, N., et al. Designing wireless powered networks assisted by intelligent reflecting surfaces with mechanical tilt. *IEEE Communications Letters*, 2022, vol. 25, no. 10, p. 3355–3359. DOI: 10.1109/LCOMM.2021.3098128

[13] NEELY, M. J. *Stochastic Network Optimization with Application to Communication and Queuing Systems*. Williston (USA): Morgan and Claypool, USA, 2010. ISBN:978-1-60845-455-6

[14] HUANG, L. NEELY, M. J. Utility optimal scheduling in energy-harvesting networks. *IEEE/ACM Transactions on Networking*, 2013, vol. 21, no. 4, p. 1117–1130. DOI: 10.1109/TNET.2012.2230336

[15] SHUMINOSKI, T., JANEVSKI, T. Lyapunov optimization framework for 5G mobile nodes with multi-homing. *IEEE Communications Letters*, 2016, vol. 20, no. 5, p. 1026–1029. DOI: 10.1109/LCOMM.2016.2540622

[16] GEORGIADIS, L., NEELY, M. J., TASSIULAS, L. Resource allocation and cross-layer control in wireless networks. *Foundations and Trends in Networking*, 2006, vol. 1, no. 1, p. 1–144. DOI: 10.1561/1300000001

[17] NEELY, M. J. Energy optimal control for time-varying wireless networks. *IEEE Transactions on Information Theory*, 2006, vol. 52, no. 7, p. 2915–2934. DOI: 10.1109/TIT.2006.876219

[18] SARIKAYA, Y., ERCETIN, O. Self-sufficient receiver with wireless energy transfer in a multi-access network. *IEEE Wireless Communications Letters*, 2017, vol. 6, no. 4, p. 442–445. DOI: 10.1109/LWC.2017.2701818

[19] GUO, L., CHEN, Z., ZHANG, D., et al. Sustainability in body sensor networks with transmission scheduling and energy harvesting. *IEEE Internet of Things Journal*, 2019, vol. 6, no. 6, p. 9633–9644. DOI: 10.1109/JIOT.2019.2930076

[20] LAN, X., CHEN, Q., CAI, L., et al. Buffer-aided adaptive wireless powered communication network with finite energy storage and data buffer. *IEEE Transactions on Wireless Communications*, 2019, vol. 18, no. 12, p. 5764–5779. DOI: 10.1109/TWC.2019.2938958

[21] PATEL, M., WANG, J. Applications, challenges, and prospective in emerging body area networking technologies. *IEEE Wireless Communications*, 2010, vol. 17, no. 1, p. 80–88. DOI: 10.1109/MWC.2010.5416354

About the Authors . . .

Slavche PEJOSKI received his bachelor, master and Ph.D. degrees from the Ss. Cyril and Methodius University in Skopje, N. Macedonia, in 2007, 2010, and 2015, respectively. He is currently an Associate Professor at Ss. Cyril and Methodius University in Skopje, N. Macedonia.

Zoran HADZI-VELKOV is a Professor of Telecommunications Engineering at the Ss. Cyril and Methodius University in Skopje, Macedonia. Between 2012 and 2014, he was visiting professor at the University of Erlangen-Nuremberg, Germany. Between 2012 and 2016, he served on the editorial board of the journal IEEE Communications Letters.

Tomislav SHUMINOSKI was born in Struga, Macedonia. He received the B.Sc. (2008), M.Sc. (2010) and Ph.D. (2016) degrees from the Faculty of Electrical Engineering and Information Technologies, University Ss. Cyril and Methodius in Skopje, N. Macedonia, where he is an Associate Professor.